BeBeC-2018-D1

Source localisation on aircraft in flight - new measurements with the DLR research aicraft Airbus 320 ATRA

Henri Siller, Wolfram Hage, Timo Schumacher
DLR Institute of Propulsion Technology, Engine Acoustics, Müller-Breslau-Str. 8, D-10623 Berlin, Germany

Abstract

Fly-over measurements with a large microphone array were performed with the Airbus A320-232 research aircraft ATRA of DLR. A large multi-arm spiral array was set up on the end of the runway of the airport. The aircraft trajectory was estimated from the vertical distance and time delays measured with an array of vertically mounted laser distance meters and GNSS trajectories recorded on board of the aircraft. Source localisation maps were obtained from a hybrid deconvolution method. The source powers in different regions of the aircraft were calculated by integrating over the source regions. The total power in the whole interrogation area matches the power in the far-field spectra, apart from contributions from sources on the ground plane which are reduced by focusing the array on the aircraft. Results from fly-overs in the same or in different configurations can be compared on the basis of the integration results and the individual sources can be ranked according to their contribution to the overall sound pressure.

1 INTRODUCTION

International regulations have lead to a substantial reduction in aircraft noise and are still being pushed forward ambitiously in Europe as well as in the US. The European Flightpath 2050 goals set by the Advisory Concil for Aviation Research and Innovation in Europe (ACARE) call for a reduction of the perceived noise emission of flying aircraft by 65 % relative to typical new aircraft in the year 2000. Other environmental goals are a 75 % reduction in carbon dioxide (CO2) emissions and a 90 % reduction in mono-nitrogen oxides (NOX) emissions.

In order to achieve these goals, the European Commission launched the Clean Sky 1 and 2 programmes as part of the Commission's Horizon 2020 Research and Innovation Programme. Clean Sky 2 comprises three Innovative Aircraft Demonstrator Platforms (IADPs), for Large Passenger Aircraft, Regional Aircraft, and Fast Rotorcraft, which are set up to develop and test flying demonstrators at full scale. The targeted sound levels will most probably not be

Figure 1: The DLR A320 research aircraft ATRA passing over the microphone array

met with the standard tube and wing configuration that is the standard of current transport aircraft designs. This raises the need for sound source localisation for aircraft in flight when new demonstrators are ready for flight testing. The technique has been developed in the beginning of this century, but will need to be improved and adapted in order to precisely analyse future aircraft configurations and propulsion systems.

The development of acoustic source localisation methods for aircraft in flight started in Europe with parallel developments at DLR in Germany ONERA in France [2**?** **?**]. Later, both organisations cooperated within the framework of the European research projects SILENCE(R) and AWIATOR in flight tests with large microphone arrays with Airbus A340 and A380 aircraft. A parallel development took place in the USA, driven mainly by Boeing for the *Quiet Technology Demonstrator (QTD)* programmes [**?** **?** **?**].

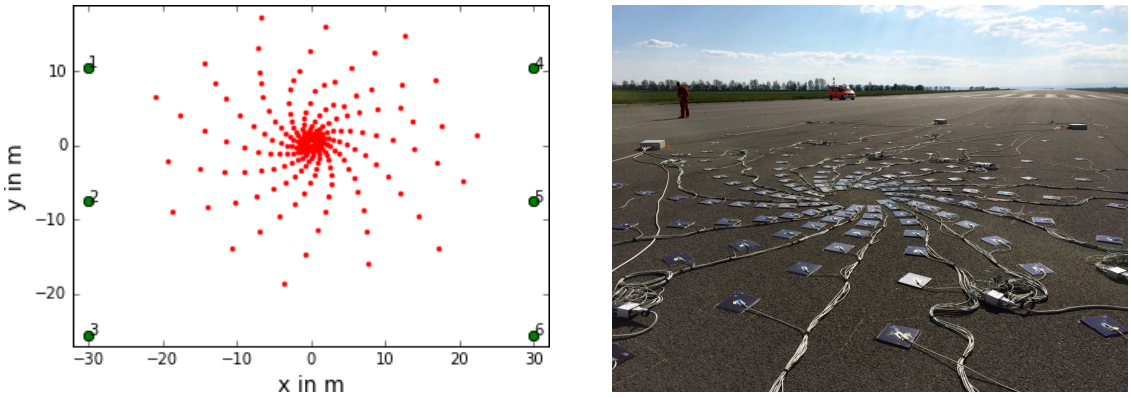

Figure 2: Left: schematic of the multi-arm spiral microphone array and the the laser distance meters (marked as green dots), right: the final set-up of the array.

The DLR engine acoustics group performed extensive fly-over noise tests with large microphone arrays in cooperation with Lufthansa within the German LuFo research programme. Fly-over tests were performed with A319 [**?** **?**], MD11 [**?**], and Boeing 747-400 [**?**] aircraft.

The experimental procedure and the data analysis are also described in Siller et al. [3]. The data analysis was initially performed with a standard beamforming in the time domain adapted to moving sources [2], but was later improved by applying a hybrid deconvolution method which post-processes the beamforming maps with the point-spread function of the microphone array in the frequency domain [1**?**]. ProSigMA, the standard code of DLR for the analysis of fly-over tests, is an implementation of this method. Fleury and Bulté [**?**] report a similar approach, which extends the analysis to different standard deconvolution algorithms, for the analysis of slat-noise from A340 fly-overs and present results that agree well with established source models. The devonvolution methods yield correct source levels that can be integrated over source regions for a quantitative analysis and a ranking of sources.

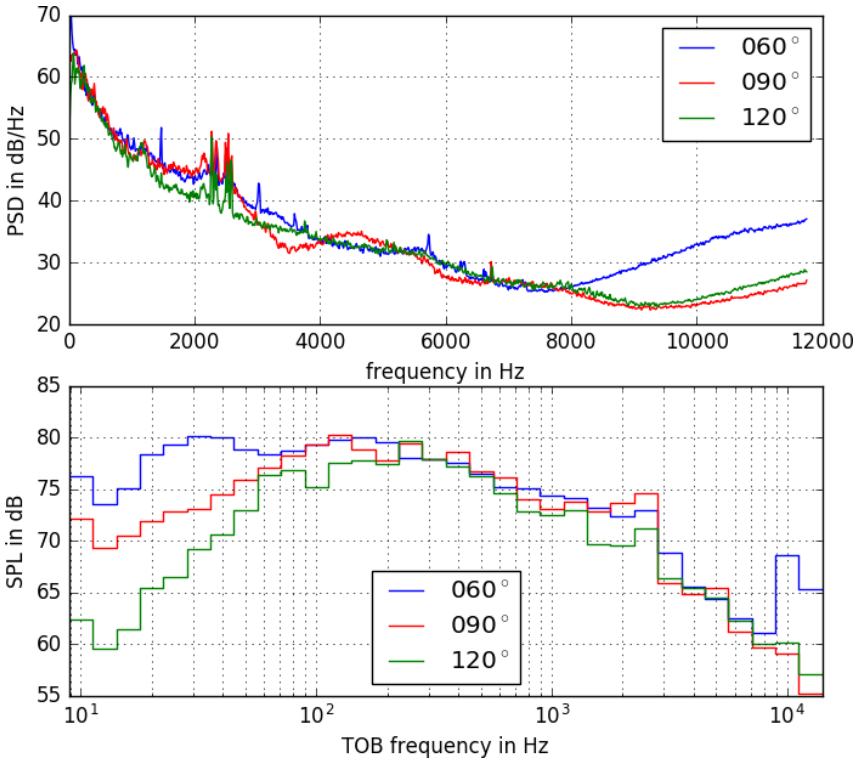

Figure 3: Doppler-compensated narrow-band spectra for fly-over 139 with the engines in flight idle and the landing gear retracted.

However, DLR has not applied this technique in fly-over measurements since the 2008 Boeing 747-400 test with Lufthansa. The existing experimental procedure and the tool chain for the analysis were revived for a new flight test with DLR research aircraft ATRA in a DLR internal research project. The data from this test are used to improve the tool chain for the analysis of individual fly-overs and the post-processing for a comparison of whole groups of fly-overs in the same configuration. This developments is driven by demands in the framework of the Clean Sky 2 programme to provide the hardware and software for fly-over tests once the IADPs are ready to launch.

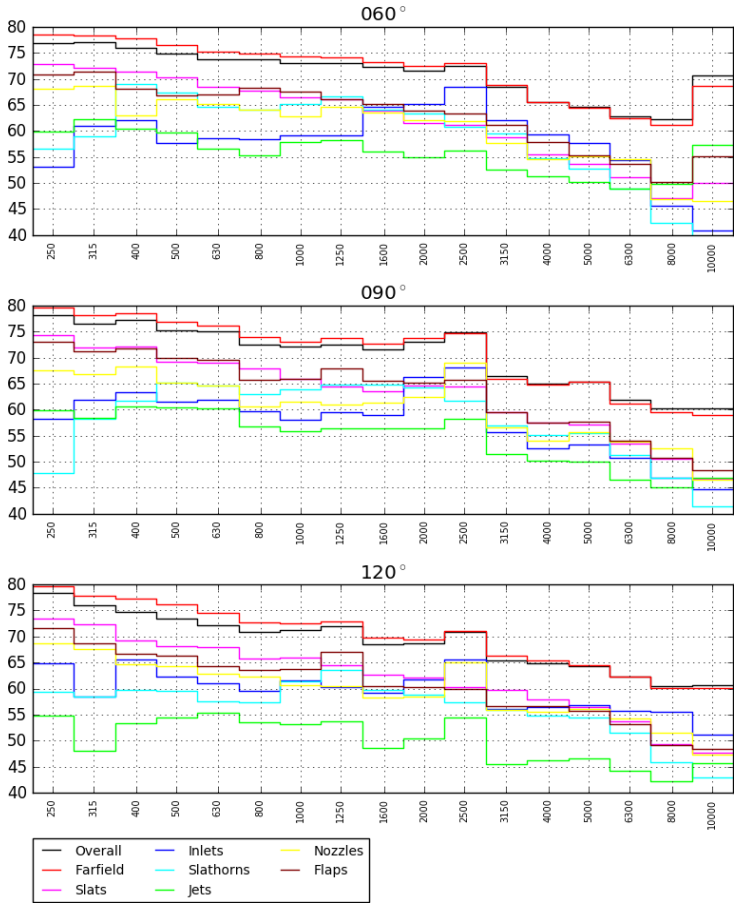

Figure 4: Spectral source break down for flyover number 139. The farfield levels are the levels of the Doppler compensated spectra from figure 3, which represent all sources from all directions while the overall level represents the integrated result of the beamforming and deconvolution which is focused on the aircraft.

2 EXPERIMENTS

Fly-over tests were performed in May 2016 at the Cochstedt airfield near Magdeburg, Germany. The research aircraft ATRA of DLR, an Airbus A320-232 with V2527-A5 engines, repeatedly passed over a microphone array in order to obtain a data base with 134 fly-overs of the aircraft in 23 different configurations with at least three repeated fly-overs in the same configuration. The experimental set-up consisted of a microphone array with 248 electret microphones set up on the end of the runway of the airport and systems of recording the flight path of the aircraft. Figures 1 and 2 illustrate the flight test with the DLR ATRA flying over the array and the set-up of the microphone array on the runway. The multi-arm spiral array had outer dimensions of 35 by 43 m and was stretched in the direction of flight in order to increase the spatial resolution when the aircraft was in approach of moving away from the array. The array centre was offset to the starboard side in the landing direction in order to avoid being on the symmetry plane of the aircraft. Flight trajectories were estimated from direct measurements with an array of laser distance meters and by recordings of Global Navigation Satellite System (GNSS) signals

on board of the aircraft which were synchronised with the microphone data by recording an IRIG-B time code together with the microphone data.

3 DATA ANALYSIS

The Doppler shift compensation and the classical beamforming were performed in the time domain using the method described by Piet et al.[2]. Sound source maps were first calculated using the standard time-domain beamforming algorithm for moving sources, which runs relatively fast. The resulting maps were used to apply small corrections to the aircraft trajectory parameters in order to compensate wind and propagation effects. When, after a couple of iterations, the aircraft was nicely centered in the source maps, the hybrid deconvolution method for moving sources by Guérin and Weckmüller [1] was applied. The resulting source maps were integrated over different source regions of the aircraft in order to derive the amplitudes of distributed sources and a ranking of the sources. The repeatability of the results can be checked by comparing the results of different fly-overs in the same configuration.

4 RESULTS

From the large data base of measured fly-overs, some examples were chosen in order to illustrate the capabilities and the work flow of the analysis. First, a single fly-over with very low engine speeds in the approach configuration will be presented in detail. Two configurations with engine speeds for take-off and climb will be presented in order to demonstrate the analysis of groups of fly-overs and the comparison of the source break down between different configurations.

4.1 Analysis of a single fly-over in approach configuration

The Doppler corrected frequency for a fly-over in a landing approach configuration with the engines in flight idle, the slats and flaps fully set ($27^\circ/40^\circ$) and the landing gear retracted are presented in figure 3. The spectra, as well as the sound source maps shown later, are calculated for emission angles $\theta = 60^\circ$, 90°, and 120° integrated over an angular range of $\Delta\theta = \pm 5^\circ$ around the nominal emission angle. The spectra are normalised to a distance of 120 m from the array centre and they are corrected for atmospheric absorption, which is why the spectrum for $\theta = 60^\circ$ shows increasing levels in the high frequency range, where the measured levels above 8 kHz actually remain constant within the noise floor of the data.

The sound source maps from the deconvolution calculations are presented in figures 5 to 7, which present the maps arranged in three vertical columns for the emission angles $\theta = 60^\circ$, 90°, and 120° for the one-third-octave bands from 315 Hz up to 8 kHz.

Point sources show very prominently in the source maps. Among the most obvious ares the slat horns at the forward roots of the wings. They are concentrated broad band sources which figure in almost all frequency bands, mainly in the forward and overhead directions. Engine tones also show up as point sources: the two last turbine stages (LPT6 and LPT7) appear in the overhead and rearward directions in the 2,0 and 2,5 kHz one-third-octave bands. Other point sources are located on the starboard sides of the forward region of the engine nacelles in the frequency bands including and above 1,6 kHz, on the port side also in the 2,0 and 2,5 kHz bands. The starboard side sources are most likely caused by cavity resonances on the ventilation holes

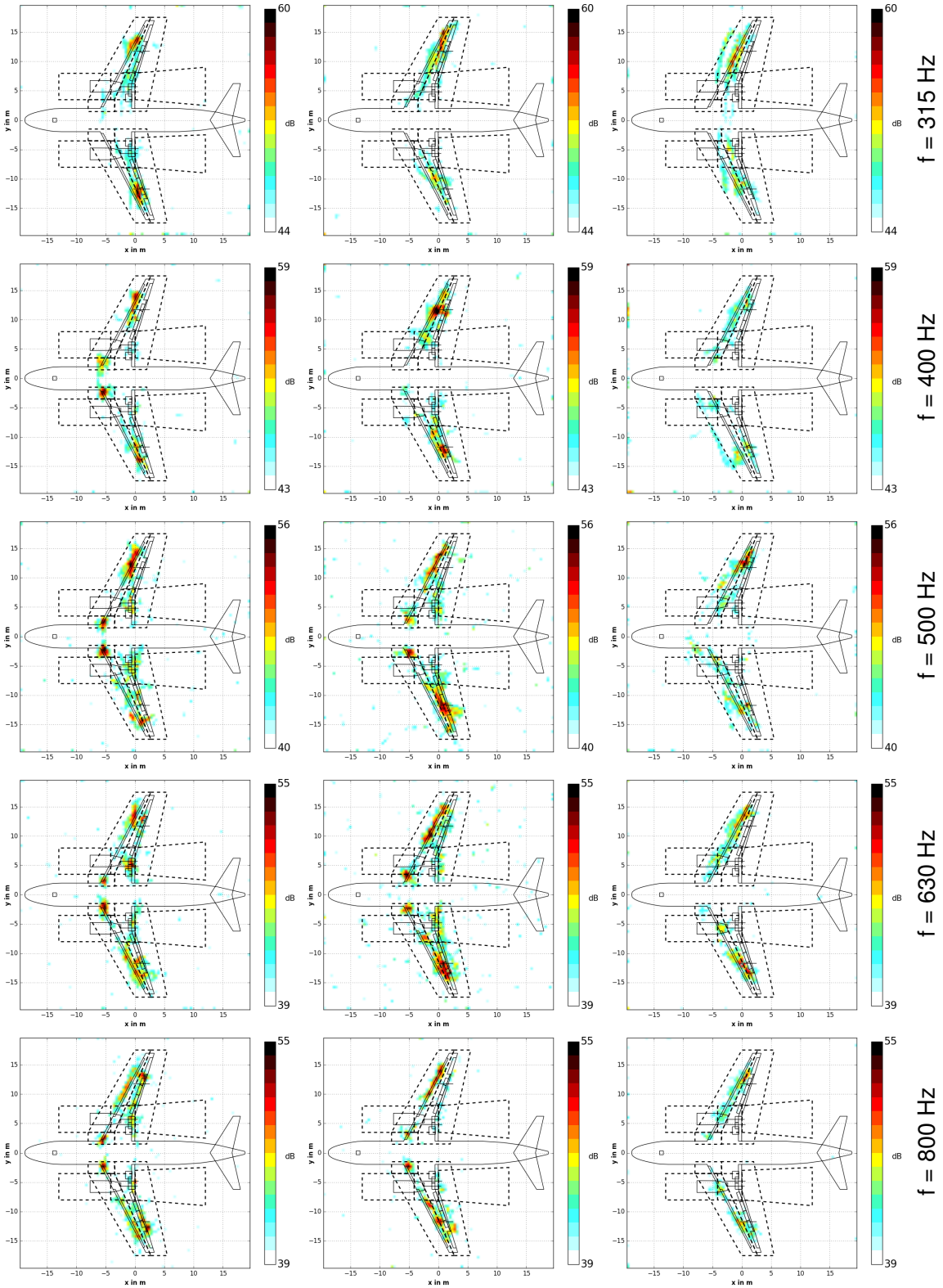

Figure 5: Source maps for the TOBs between 315 and 800 Hz for flyover number 139.

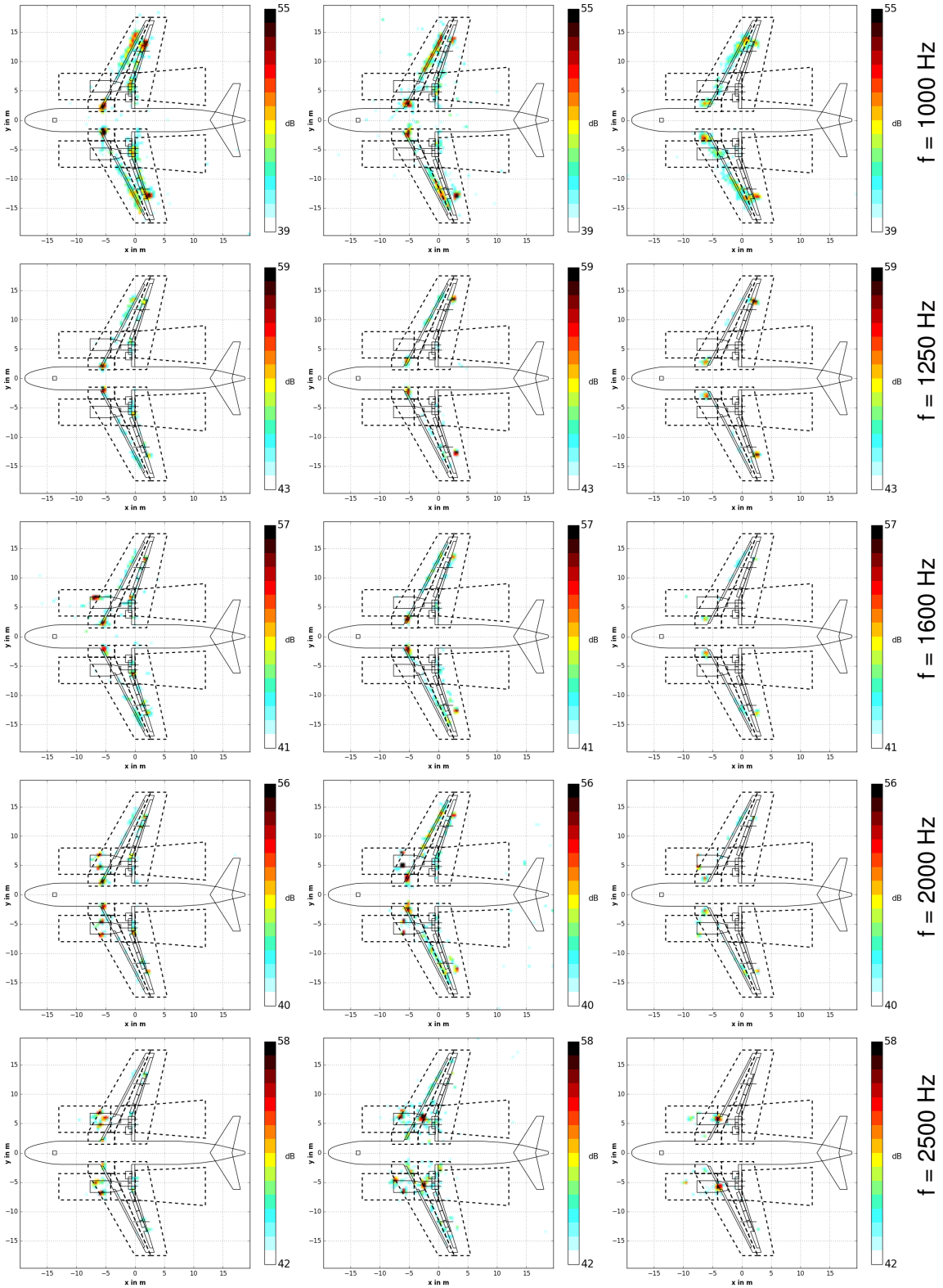

Figure 6: Source maps for the TOBs between 1000 and 2500 Hz for flyover number 139.

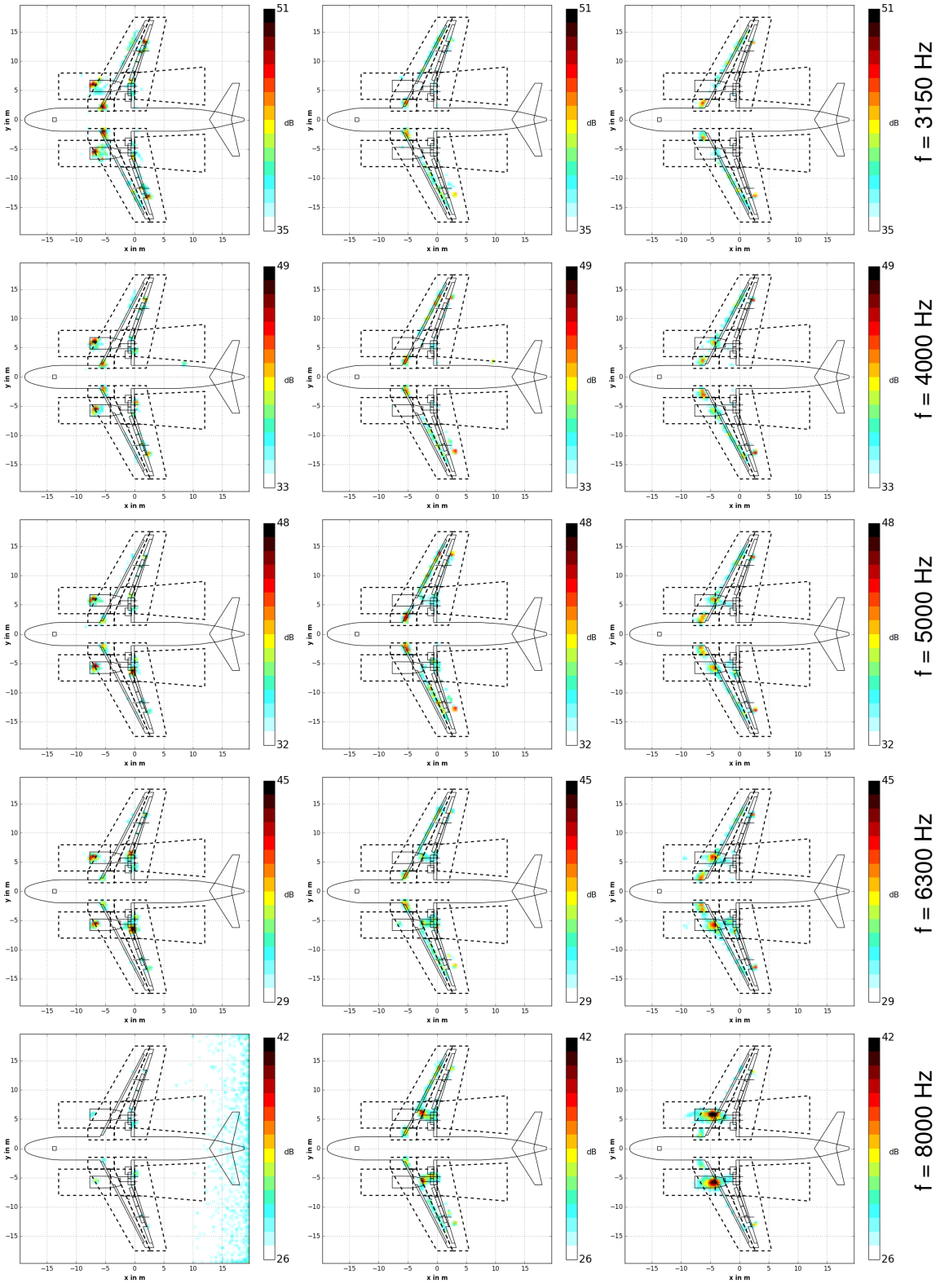

Figure 7: Source maps for the TOBs between 3150 Hz and 8 kHz for flyover number 139.

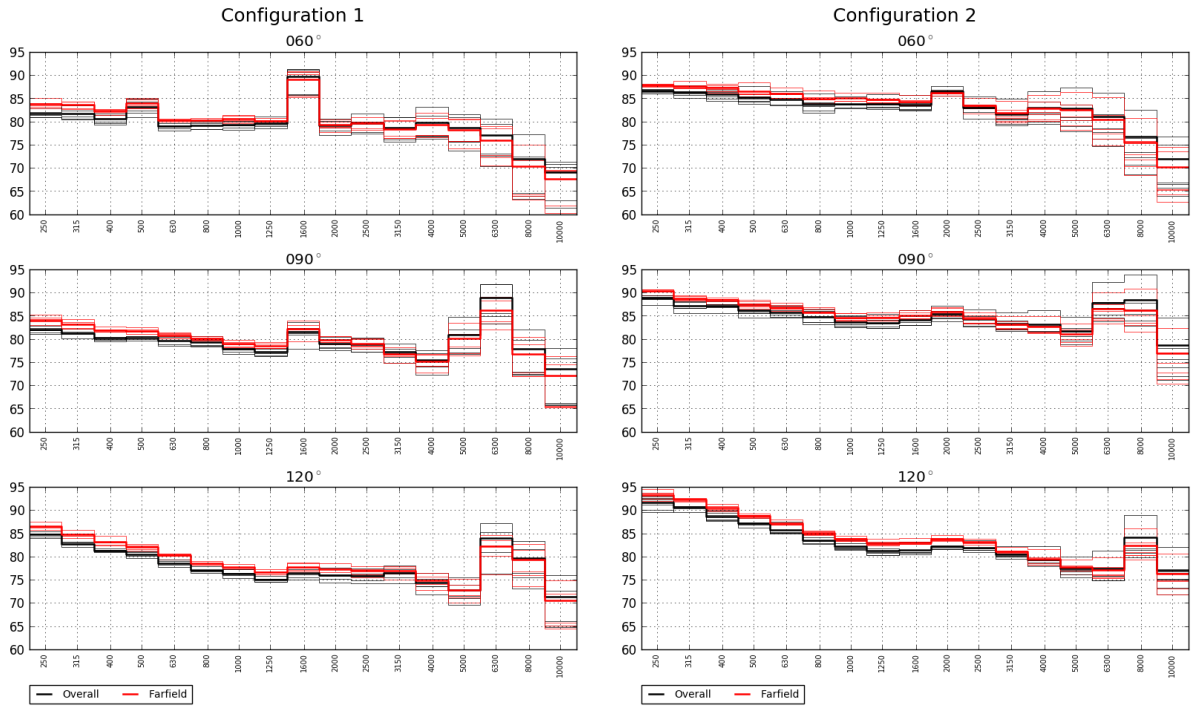

Figure 8: Farfield and overall integrated powers for the individual fly-overs in the climb (1) and take-off (2) configurations. The narrow lines represent the data of the individual fly-overs, the thick solid lines the energetic averages of all fly-overs in the same configuration.

of the de-icing system. The fan blade passing frequency of the engines fan stage (BPF1) is 578 Hz, which belongs into the 630 Hz one-third-octave band. At this fan speed, the BPF1 tone is cut-off and appears neither in the frequency spectra nor in the source maps.

Very strong distributed sources like the slats along the wing leading edges and the flaps along the trailing edges can also be clearly seen in the source maps. Both are broadband sources and especially the slats stand out very clearly in the maps. The flap side edges figure as two strong point sources in the outer region of the wings, especially in the higher frequency bands.

When the source powers from the deconvolution results are integrated over different source regions, the contributions of the different source regions to the overall sound emitted by the aircraft can be estimated. Figure 4 presents the spectra of the source break down of fly-over number 139 shown in figures 3 and 5 to 7. The far-field specta are simply the Doppler-compensated frequency spectra calculated straight from the data without further array processing, the overall sound pressure spectrum results from the integration of the powers over the whole cartesian grid in the source plane with 99×99 grid points that are separated by $\Delta x = \Delta y = 0,4\,\mathrm{m}$. The overall levels are usually lower than the far-field levels because the focusing of the array on the source plane suppresses sources on the ground, like nearby traffic or electrical generators.

The slats are the loudest source over a wide range of frequencies below 1 kHz, followed by the sources in the flap region. In the 1250 Hz band, the flap side edges are the strongest source in that band for $\theta = 90°$ and 120°. Engine sources are only of secondary importance with the engines running in flight idle. The engine inlet and the jet are among the weakest sources in this

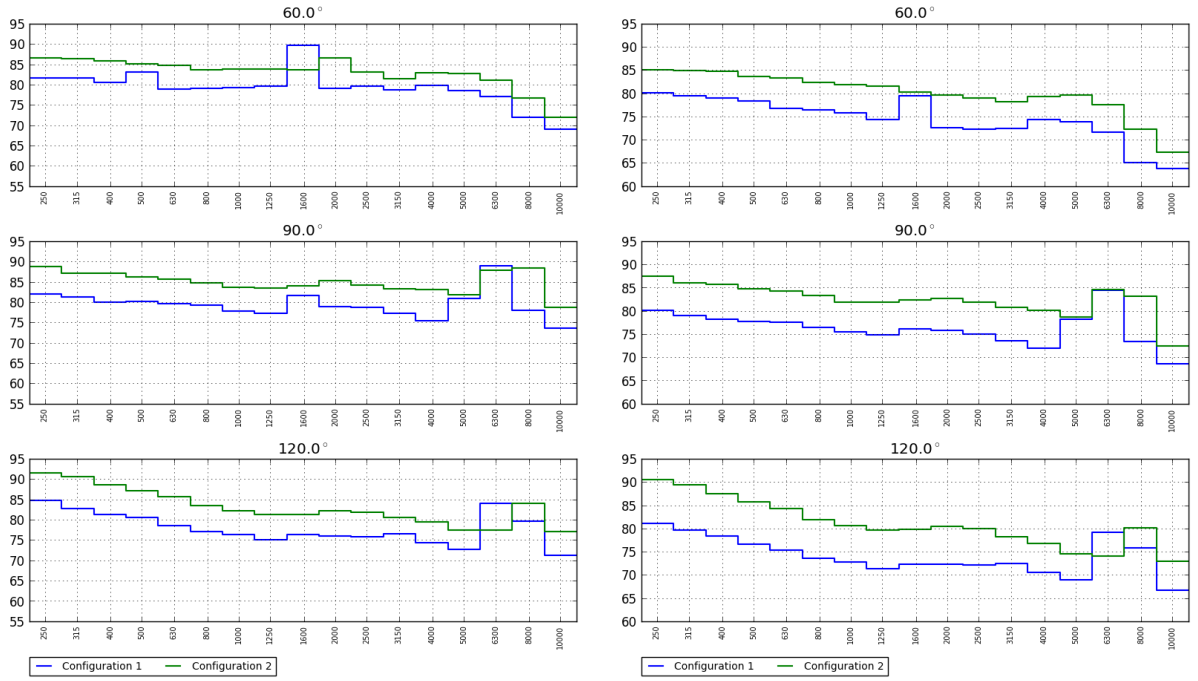

Figure 9: Comparison of the averaged fly-overs in the climb (1) and take-off (2) configurations. Result of the power integration over the whole interrogation grid (left) and the nozzle and jet noise regions only (right).

configuration. The engine nozzle region is difficult to separate from the slat and flaps regions in that area of the wing span and a certain amount energy will be accounted for in the wrong region. The nozzle is, however, an important source in the 2,0 and 2,5 kHz bands which contain the low-pressure turbine tones generated in the last two stages.

4.2 Comparative analysis of multiple fly-overs in two engine noise configurations

The effect of engine noise at take-off engine speeds can be studied by comparing two configurations for take-off and climb. The engine speeds are nominally $N1 = 81\,\%$ and $N1 = 91\,\%$, respectively. Both configurations have in common that the slats and flaps setting is $22°/20°$, the landing gear is retracted, and the nominal speed is about $65\,\mathrm{m/s}$. In configuration 1 (climb), with an engine shaft speed of $N1 = 81\,\%$, five different fly-overs were recorded, in configuration 2 (take-off) with $N1 = 91\,\%$, six fly-overs. Figure 8 shows the farfield spectra of each fly-over as a thin line and the energetic average of all fly-overs in the same configuration as a thick line of the same colour for both configurations (number 1 on the left hand side and number 2 on the right hand side of the figure). The repeatability of the fly-overs is very good up to frequencies of over 4 kHz, where the correction of the atmospheric absorption gains increasing importance and may pull up levels when the signals approach the noise floor.

The most prominent features of the spectra are the tone of the engine fan stage blade passing frequency (BPF1) and the low-pressure turbine tones from the last two turbine stages, LPT6 and LPT7. In climb, with $N1 = 81\,\%$, the BPF1 has a frequency of about 1670 Hz and falls into the 1,6 kHz one-third-octave band. The turbine tones LPT6= 6400 Hz and LPT7= 6700 Hz

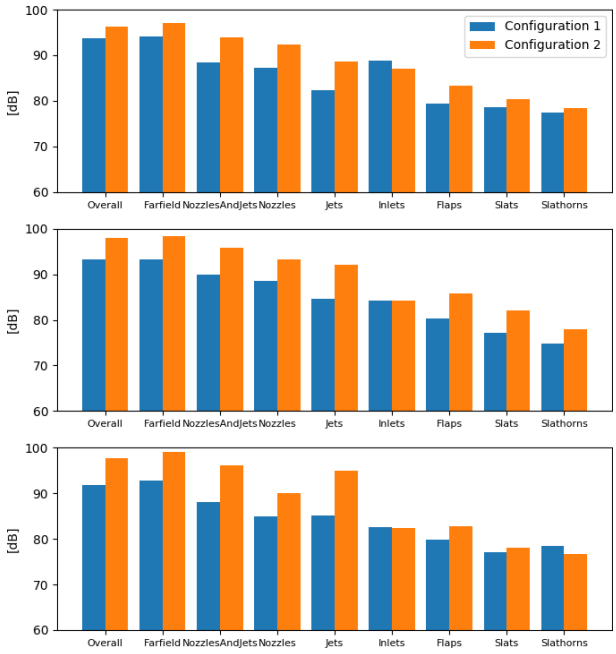

Figure 10: Sound pressure levels integrated over all one-third-octave bands for configuration 1 (climb) and configuration 2 (take-off). Top: $\theta = 60°$, centre: $\theta = 90°$, and bottom: $\theta = 120°$.

both fall into the 6,3 kHz one-third-octave band. In the take-off configuration, the engine speed is higher with $N1 = 91\,\%$ and the BPF1 is at about 1880 Hz, which is contained in the 2,0 kHz one-third-octave band, while the turbine tones are LPT6= 7270 Hz and LPT7= 7600 Hz, both falling into the 8,0 kHz one-third-octave band. These tones can be found in the graph on the left hand side of figure 9, which presents a direct comparison of the averaged results for each configuration for the power integrated over the whole interrogation grid. The BPF1 tone in climb is actually louder than in take-off, while the turbine noise remains at almost equal levels (but moves up in frequency from the 6,3 kHz into the 8,0 kHz band). Additional buzz-saw tones show up in the 500 Hz one-third-octave band.

The graph on the right hand side of figure 9 presents the total rearward engine noise contribution that is obtained from integrating over the engine nozzle and jet regions. Comparing the left and right hand side plots in figure 9, reveals that the take-off (configuration 2) is dominated by noise from the nozzles and jets in the rear arc at $\theta = 120°$. When the aircraft is overhead, this is still the case over most of the frequency range. In the forward arc, at $\theta = 60°$, the balance is different and sources from the inlet region become more important.

The engine BPF1 tone also propagates through the bypass duct of the engine as rearward fan noise. However, it is only for the climb configuration in the forward arc, at $\theta = 60°$, that it is strong enough above the jet noise that it shows up in the spectrum of the nozzle and jet regions.

The absolute values of tonal levels, however, have to be treated with caution because the hybrid deconvolution scheme assumes broad band sources and cannot be expected to yield correct tonal amplitudes.

The results of the power integration can be used to obtain a source ranking. Figure 10 presents a comparison of the amplitudes in the different source regions for the climb and take-off con-

figurations. This shows that the order of the contribution to the overall sound pressure level at each emission angle is slightly different between the climb and the take-off configurations: in climb, the BPF1 is actually louder than at take-off although the engine speed is just over 10 % lower. The sources in the rearward region of the engine, including the region where interaction between the jet and the wing flap occurs, are stronger than the jet noise in the forward and overhead direction. In the rear arc, however, the jet noise dominates over the nozzle region. The inlet region is only important in the forward arc, in the overhead and rear arc, they rank on a similar level as the airframe noise sources in the slat, flap and slat horn regions, which are all at least 12 dB below the overall sound level.

5 CONCLUSIONS

Data from a flight test with the DLR research aircraft ATRA and a large microphone array has been presented. The data have been analysed using a tool chain based on the existing ProSigMA code, that implements a hybrid beamforming and deconvolution method, and new post-processing routines for the source integration and ranking of source regions according to their contribution to the overall sound level. A fly-over in an approach configuration with retracted landing gear and the engines in flight idle has been presented in detail with the frequency spectra and the sound source maps. For two engine noise configurations with engine speeds in climb and take off with multiple fly-overs per configuration, the averaged results of the deconvolution analysis and the source integration results averaged over each configuration were compared. The spectra of the individual source regions were compared and a ranking of the sources based on the overall sound pressure levels in each source region were presented.

Acknowledgements

This project has received funding from the Clean Sky 2 Joint Undertaking under the European Union's Horizon 2020 research and innovation programme under grant agreement No. CS2–LPAGAM–2014–2015–01

6 REFERENCES

[1] V. Fleury and J. Bulté. "Extension of deconvolution algorithms for the mapping of moving acoustic sources." *Hournal of the acoustic society of America*, 129(1417), 2011.

[2] S. Guérin and U. Michel. "Aero-Engine Noise Investigated from Flight Tests." In *12th AIAA/CEAS Aeroacoustics Conference, Cambridge, MA, 8-10 June 2006*. 2006.

[3] S. Guérin and H. Siller. "A Hybrid Time-Frequency Approach for the Source Localization Analysis of Acoustic Fly-over Tests." In *14th CEAS/AIAA Aeroacoustics Conference, Vancouver, British Columbia, Canada, 5-7 May 2008*. 2008.

[4] S. Guérin and C. Weckmüller. "Frequency-domain reconstruction of the point-spread function for moving sources." In *Proceedings on CD of the 2nd Berlin Beamforming Conference, 19-20 February, 2008*. GFaI, Gesellschaft zu Förderung angewandter Informatik e.V., Berlin, 2008. ISBN 978-3-00-023849-9. URL http://www.bebec.eu/Downloads/BeBeC2008/Papers/BeBeC-2008-14_Guerin_Weckmueller.pdf.

[5] U. Michel, B. Barsikow, B. Haverich, and M. Schüttpelz. "Investigation of airframe and jet noise in high-speed flight with a microphone array." In *3rd AIAA/CEAS Aeroacoustics Conference, Atlanta, Ga, May 12-14, 1997*. 1997. URL http://bebec.eu/Downloads/Beamforming_Repository/AIAA-1997-1596_Michel_etal.pdf.

[6] J.-F. Piet and G. Élias. "Airframe noise source localization using a microphone array." In *3rd AIAA/CEAS Aeroacoustics Conference, Atlanta, Ga, May 12-14, 1997*. 1997. URL http://pdf.aiaa.org/preview/1997/PV1997_1643.pdf.

[7] J.-F. Piet, U. Michel, and P. Böhning. "Localization of the acoustic sources of the A340 with a large phased microphone array during flight tests." In *8th AIAA/CEAS Aeroacoustics Conference, Breckenridge, Co, 17-19 June 2002*. 2002. URL http://pdf.aiaa.org/preview/CDReadyMAERO02_554/PV2002_2506.pdf.

[8] P. Sijtsma and R. W. Stoker. "Determination of absolute contributions of aircraft noise components using fly-over array measurements." In *10th AIAA/CEAS Aeroacoustics Conference, May 10-12, 2004, Manchester, Great Britain*. 2004. AIAA 2004-2958.

[9] H. Siller. "Localisation of sound sources on aircraft in flight." In *Proceedings on CD of the 4th Berlin Beamforming Conference, 22-23 February 2012*. GFaI, Gesellschaft zu Förderung angewandter Informatik e.V., Berlin, 2012. ISBN 978-3-942709-04-0. URL http://bebec.eu/Downloads/BeBeC2012/Papers/BeBeC-2012-01.pdf.

[10] H. Siller, M. Drescher, G. Saueressig, and R. Lange. "Fly-over source localisation on a Boeing 747-400." In *Proceedings on CD of the 3rd Berlin Beamforming Conference, 24-25 February, 2010*. 2010. URL http://bebec.eu/Downloads/BeBeC2010/Papers/BeBeC-2010-13.pdf.

[11] H. Siller and U. Michel. "Buzz-Saw Noise Spectra and Directivity from Flyover Tests." In *8th AIAA/CEAS Aeroacoustics Conference, Breckenridge, Co, 17-19 June 2002*. 2002. URL http://pdf.aiaa.org/preview/CDReadyMAERO02_554/PV2002_2562.pdf.

[12] H. Siller, U. Michel, C. Zwiener, and G. Saueressig. "Reduction of Approach Noise of the MD-11." In *12th AIAA/CEAS Aeroacoustics Conference (27th AIAA Aeroacoustics Conference), Cambridge, Massachusetts, May 8-10, 2006*. 2006. URL http://pdf.aiaa.org/preview/CDReadyMAERO06_1268/PV2006_2464.pdf.

[13] R. Stoker and Y. Guo. "Airframe Noise Source Locations of a 777 Aircraft in Flight and Comparison with Past Model-Scale Tests." In *10th AIAA/CEAS Aeroacoustics Conference, Manchester, United Kingdom, 10-12 May 2004*. 2004.

[14] R. W. Stoker, Y. Guo, C. Streett, and N. Burnside. "Airframe Noise Source Locations of a 777 Aircraft in Flight and Comparisons with Past Model-Scale Tests." In *9th AIAA/CEAS Aeroacoustics Conference and Exhibit, Hilton Head, South Carolina, May 12-14, 2003*. 2003.